frontiers | Frontiers in Energy Research

TYPE Original Research
PUBLISHED 04 January 2023
DOI 10.3389/fenrg.2022.1007566

OPEN ACCESS

EDITED BY
Hui Shang,
China University of Petroleum, Beijing, China

REVIEWED BY
Xiqiang Zhao,
Shandong University, China
Yang Jiao,
Shanghai Ocean University, China

*CORRESPONDENCE
Shumeng Yin,
13076033921@139.com

SPECIALTY SECTION
This article was submitted to Process and Energy Systems Engineering, a section of the journal Frontiers in Energy Research

RECEIVED 30 July 2022
ACCEPTED 12 September 2022
PUBLISHED 04 January 2023

CITATION
Yin S (2023), Effect of metal slots on the heating uniformity of multisource cavity microwave.
Front. Energy Res. 10:1007566.
doi: 10.3389/fenrg.2022.1007566

Effect of metal slots on the heating uniformity of multisource cavity microwave

Shumeng Yin[1,2]*

[1]SINOPEC Research Institute of Safety Engineering Co, Ltd, Qingdao, China, [2]State Key Laboratory of Safety and Control for Chemicals, SINOPEC Research Institute of Safety Engineering Co, Ltd, Qingdao, China

Microwave heating as a new type of heating has been widely used in numerous fields; however, microwave heating in multi-source cavity still poses several problems, including non-uniformity, low efficiency, restriction of the heating object, and "thermal runaway", thus limiting the application of microwave energy. This study adopts a method to place a slotted layer in the cavity such that the energy can be radiated uniformly to improve the heating uniformity. The distribution of the electric field in the cavity is optimized by changing the arrangement and size of the slots in the slot layer. The effects of the slot arrangements are elucidated, and experiments are performed to study the real-life application of the slot arrangements. The results show that these metal slots are effective in improving the uniformity and efficiency of multisource cavity heating.

KEYWORDS

high efficiency, metal slots, microwave heating, uniformity, multisource cavity

1 Introduction

Microwaves are electromagnetic waves with frequencies ranging from 300 MHz to 3,000 GHz. With continuous research, microwaves are widely used in industrial heating, such as microwave petroleum pyrolysis (Khelfa et al., 2020; Kumar et al., 2020; Taheri-Shakib and Kantzas, 2021; Zhu et al., 2021), auxiliary pyrolysis, coal desulfurization and drying (Li et al., 2019; Liao et al., 2019; Si et al., 2019; Cai et al., 2021; Lichao and Xiaoyan, 2022; Yucen et al., 2022; Zhu et al., 2022), and microwave crushing (Hassani et al., 2016; Hartlieb et al., 2018; Chen et al., 2021). The size of traditional electrically large microwave heating equipment is similar to the wavelength, which makes the electric field distribution in the cavity non-uniform. In addition to their size, their cavity wall reflections, port reflections, and other restrictions result in non-uniform temperature distribution in the cavity and inefficient heating. Therefore, improving the efficiency and uniformity of microwave heating has become a key issue in current microwave research (Shan, 2020; Gu et al., 2022; Shen et al., 2022; Suhail et al., 2022).

To solve the problems of non-uniformity and low efficiency of microwave heating, several scholars and experts in this field have conducted extensive research. Their studies show that changing the distributions of the electromagnetic field and heated material in the cavity can effectively improve the uniformity of microwave heating.

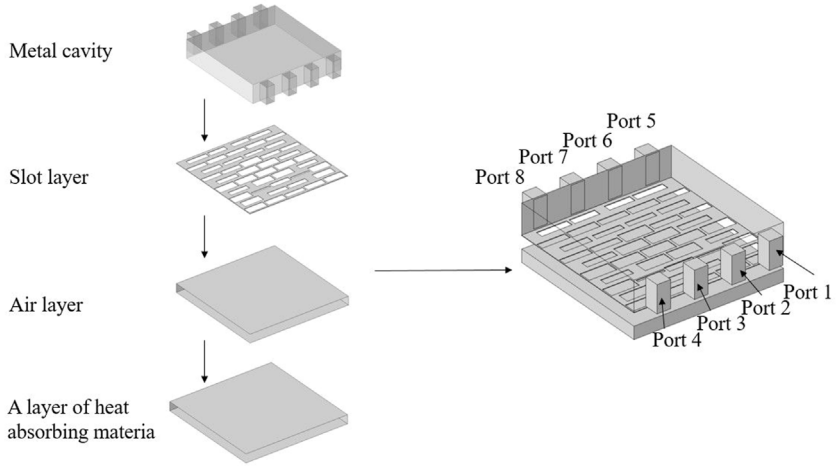

FIGURE 1
Model geometry.

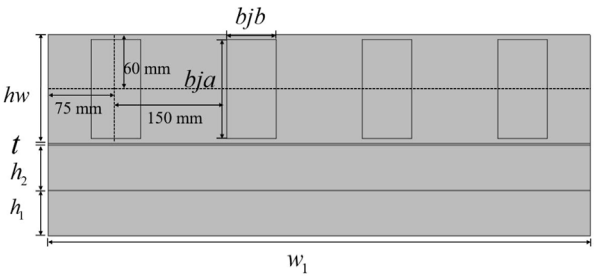

FIGURE 2
Waveguide distribution diagram.

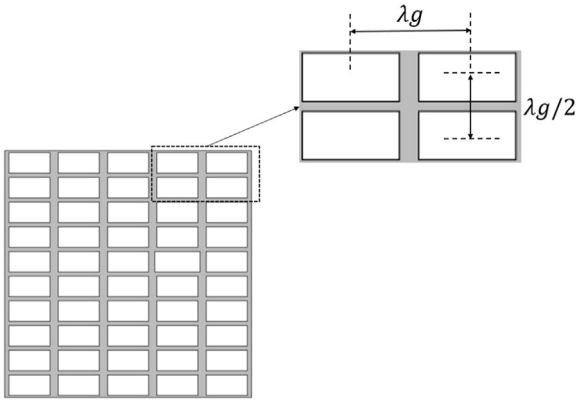

FIGURE 3
Schematic of a uniform slot arrangement.

TABLE 1 Material parameters.

Properties	Air	Heat-absorbing materials
Relative permittivity	1	3.6–0.09 j
Relative magnetic permeability	1	1
Thermal conductivity/W/m•K	-	20
Conductivity/S/m	0	0
Density/kg/m^3	-	580
Isobaric heat capacity/J/kg•K	-	960

For example, using a stirring mode, the electromagnetic field distribution within the cavity can be altered to ensure the uniformity of heating by designing a stirrer that oscillates either periodically or non-periodically (Cuccurullo et al., 2017; Ye et al., 2019; Wang Y et al., 2021). A rotating lifting turntable can be used to rotate the sample such that it absorbs microwaves uniformly in all directions (Geedipalli et al., 2007; Dinani et al., 2020; Ye et al., 2021). In addition, because heating performance is highly dependent on microwave frequencies (Tang et al., 2018; Yang et al., 2019; Wu et al., 2021), certain frequencies can help improve the heating performance more than others; hence, it is possible to improve the heating performance by selecting specific frequencies. When the microwave frequency is fixed, the position and shape of the ports can be changed. For example, when two radiation ports rotate around their axes, the heating efficiency at different angles is analyzed, and subsequently, the effective angle of the radiation port is determined (Luan et al., 2016; He et al., 2020; Wang C et al., 2021). Additionally, the continuous control of the input power

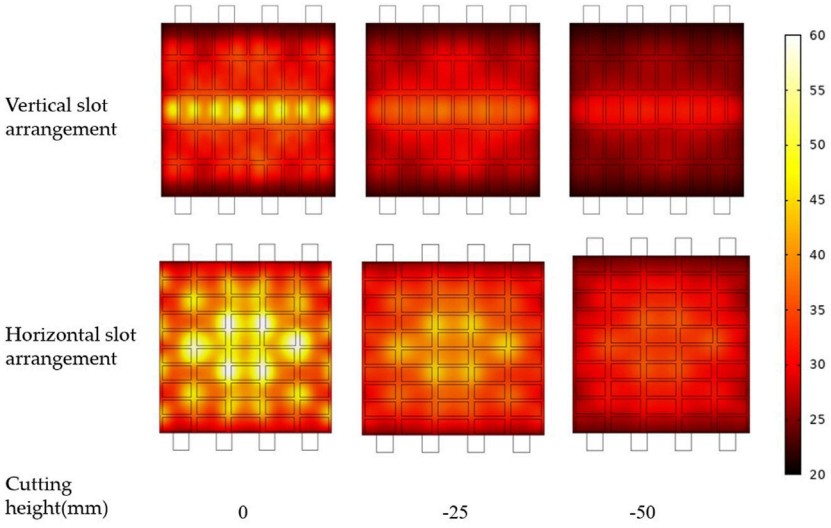

FIGURE 4
Temperature distribution in the cross section of heat absorbing material for vertical and horizontal slot arrangement.

TABLE 2 Heating results of the vertical and horizontal slot arrangements.

Slot arrangement	Average body temperature (K)	COV	*RA* (%)
Vertical	302.2	0.371	19.0
Horizontal	307.9	0.305	32.0

of multiple microwave sources can change the electromagnetic field in the cavity, improve the uniformity of microwave heating, and optimize the utilization of microwave energy (Bae et al., 2017; Ahn et al., 2019; Ahn et al., 2020). In high-power microwave heating, a waveguide slot radiator is often employed to achieve microwave heating. For example, owing to the phase difference between the horizontal and vertical slots in an orthogonal slot-loading array waveguide, the electric field distributed in different directions becomes uniform, thus improving heating uniformity (Razmhosseini and Vaughan, 2017). Since our research needs to meet the high power requirements, we choose to achieve uniform microwave heating based on waveguide slot radiators. There are other methods for improving the uniformity of microwave heating (Li et al., 2020). Although the energy utilization of microwave heating will improve when multiple microwave sources are introduced, the phenomena of mutual coupling between the ports, reflection from the inner wall of the cavity, and appearance of cold spots during heating, which can result in non-uniform heating, are problems that are yet to be solved.

Herein, we propose a method to add a slot layer in the cavity to radiate energy uniformly to improve the heating uniformity and efficiency. In the absence of slot structure, electromagnetic energy will be reflected back at the feed port or be quickly absorbed, and the load in the middle of the cavity will not absorb the energy. When a metal slot layer is added, microwaves enter the cavity through the port, and due to the size of the metal slot, the microwaves resonate near the operating frequency and are then secondarily radiated to the material to be heated by the slot, thus achieving high efficiency. At the same time, the structure of the slot changes the electric field distribution in the cavity, thus making the electric field more uniform and achieving high uniformity. The distribution of the electric field in the cavity was optimized by adjusting the size and arrangement of the rectangular slots in the slot layer to improve heating uniformity. Herein, Section 2 describes the model and analyzes the effects of the size and arrangement of the rectangular slots in the slot layer on the uniformity; additionally, experiments are conducted to verify the accuracy of the model. Section 3 provides a summary of the work done in this paper.

2 Materials and methods

2.1 Geometric modeling

The model was built in COMSOL Multiphysics software (5.6, COMSOL Inc., Stockholm, Sweden) (Figure 1, 2) and divided into four layers. The metal cavity made up the first layer [length (w_1) = 600 mm, width (w_2) = 600 mm, height (hw) = 120 mm, and thickness (t) = 2 mm). As shown in the figure, there were eight WR430 microwave ports, which were symmetrically

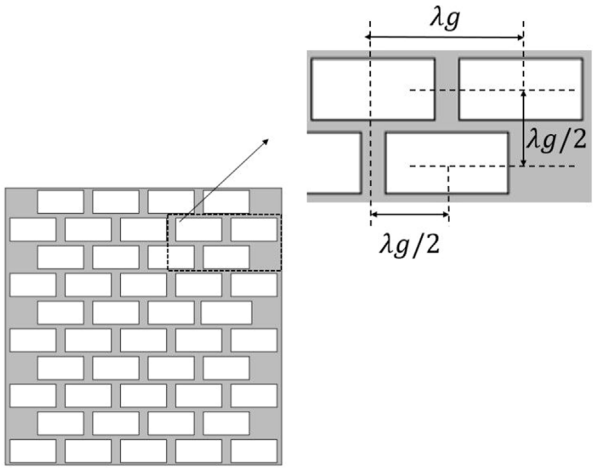

FIGURE 5
Schematic of a staggered slot arrangement.

located on both sides of the cavity. The second layer was the slot layer (length (w_1), width (w_2), and height (t)]. Layer three was an air layer (length (w_1)), width (w_2), and height (h_2) = 50 mm). Finally, layer 4, was a layer of heat-absorbing material. The specific composition of the heat-absorbing material is 80% SiC and 20% bentonite by sintering, whose dielectric constants are referred to Table 1. (length (w_1), width (w_2), and height (h_1) = 50 mm). The number, size, and arrangement of the slots in the slot layer were designed such that electromagnetic waves could be radiated through the slots and air layer to the heat-absorbing material layer to allow the heating of the material. The excitation mode of the ports (TE_{10}mode) was determined to be at 2.45 GHz, with an input power of 800 W per port and the heating time was 120 s.

2.2 Control equations

We used the coupling of the electromagnetic field and solid heat transfer modules as well as a system of Maxwell's equations to study the distribution of the electromagnetic field using the COMSOL Multiphysics software.

$$\begin{aligned} \nabla\times\vec{H} &= \vec{J} + \varepsilon\frac{\partial\vec{E}}{\partial t} \\ \nabla\times\vec{E} &= -\frac{\partial\vec{B}}{\partial t} \\ \nabla\cdot\vec{B} &= 0 \\ \nabla\cdot\vec{D} &= \rho_e \end{aligned} \tag{1}$$

where $\vec{E}$ is the electric field strength (V/m), and $\vec{H}$ is the magnetic field strength (A/m), and ε is the permittivity (F/m), and $\vec{D}$ is the electric displacement vector (C/m^2), and $\vec{J}$ is the conduction current density (A/m^2), and $\vec{B}$ is the magnetic induction strength (Wb/m^2), and ρ_e is the charge body density (C/m^3), and t is a time variable (s).

Electromagnetic energy loss is calculated using the following electromagnetic loss formula:

$$Q_e = \frac{1}{2}\omega\varepsilon_0\varepsilon''\left|\vec{E}\right|^2 \tag{2}$$

where Q_e is the electromagnetic energy loss (W); ω is the angular frequency (rad/s); ε_0 is the vacuum permittivity, and ε'' is the imaginary part of the permittivity.

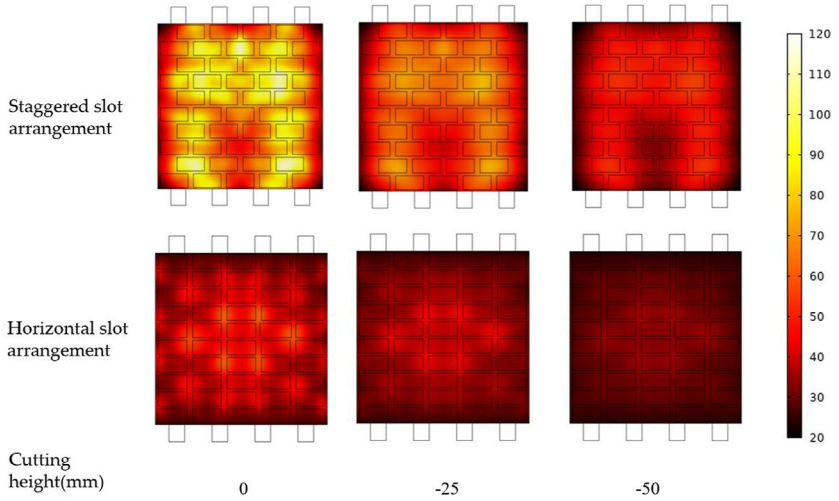

FIGURE 6
Temperature distribution of cross sections of heat absorbing materials for staggered and horizontal slot arrangements.

TABLE 3 Heating results of the staggered and uniform slot arrangements.

Slot arrangement	Average body temperature (K)	COV	*RA* (%)
Staggered	333.7	0.28	87.6
Uniform	307.9	0.305	32.0

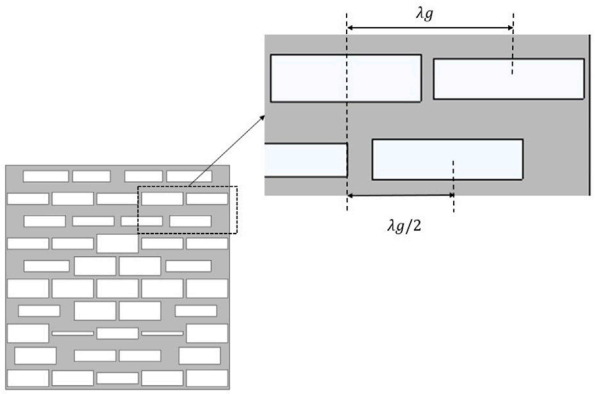

FIGURE 7
Schematic of the optimized slot arrangement.

The temperature distribution of the heat-absorbing material and heated model can be calculated using the following heat conduction equation.

$$\rho C_p \frac{\partial T}{\partial t} - k\nabla^2 T = Q_e \tag{3}$$

where ρ is the density of the substance (kg/m^3). C_p is the atmospheric heat capacity of the substance $(J/(kg \cdot K))$. k is the thermal conductivity of the substance $(W/(m \cdot K))$, and T is temperature (K).

2.3 Initial values and boundary conditions

The metal waveguide and cavity wall were considered perfect electrical conductors when the electromagnetic field distribution was calculated in the model such that the normal electric field components on the metal waveguide and the cavity wall were zero, which satisfies the following equation.

$$\vec{n} \times \vec{E} = 0 \tag{4}$$

where $\vec{n}$ is the unit normal vector of the corresponding surface.

The electromagnetic waves were transmitted into the cavity through eight excitation ports. As the electromagnetic wave enters the cavity from eight ports, it is set as the excitation port, and the mode is the TE_{10} mode. During simulation, a solid heat transfer analysis of the heated object is performed, the heat exchange around the heated object is considered, and the initial boundary is set to the heat flux, which satisfies the following equation.

$$q_0 = h \cdot (T_{ext} - T) \tag{5}$$

where q_0 is the convective heat flux, T_{ext} is the external temperature (293.15 K), and h is the heat transfer coefficient $(300W/(m^2 \cdot K))$. The initial temperature of the heated material was set at 293.15 K.

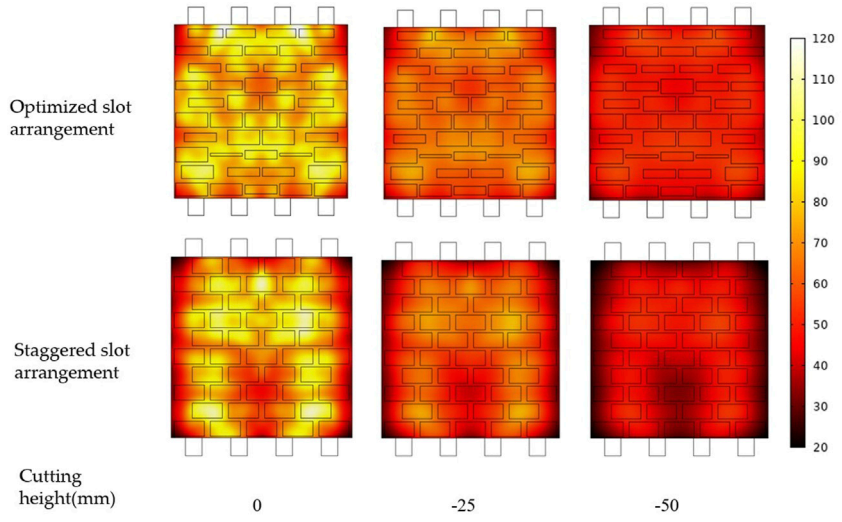

FIGURE 8
Temperature distribution of cross sections of heat absorbing materials for optimized and non-optimized slot arrangements.

TABLE 4 Heating results of the optimized and non-optimized slot arrangements.

Slot arrangement	Average body temperature (K)	COV	*RA* (%)
Optimized	336.3	0.22	95.7
Non-optimized	333.7	0.28	87.6

TABLE 5 Effect of variation of the slot width on the heating effect.

Variation of slot size	Average body temperature (K)	COV	*RA* (%)
Increased by 1 mm	336.4	0.2258	95.9
Unchanged	336.3	0.2262	95.8
Reduced by 1 mm	336.1	0.2267	95.7

TABLE 6 Effect of variation of the slot length on the heating effect.

Variation of slot size	Average body temperature (K)	COV	*RA* (%)
Increased by 1 mm	336.5	0.2391	96.6
Unchanged	336.2	0.2262	95.8
Reduced by 1 mm	335.9	0.2443	94.5

2.4 Material parameters

The parameters of the heat-absorbing materials involved in this model using the COMSOL Multiphysics software are listed in Table 1.

3 Results and discussion

3.1 The effects of horizontal and vertical slots on microwave heating

The coefficient of temperature variation (COV) is used to measure the non-uniformity of the temperature distribution. The calculation method is the standard deviation of the temperature rise at each position of the sample divided by the average value of the temperature rise at each position. The COV could be expressed as:

$$COV = \sqrt{\frac{\sum_n (T_i - T_a)^2}{n}} \Big/ (T_a - T_0) \quad (6)$$

where T_i is the point temperature of the selected region, T_a is the average temperature of the selected region, n is the total number of the point of it, and T_0 is the initial average temperature.

Heating efficiency is usually measured by the load's absorption rate for microwaves. The absorption rate could be expressed as:

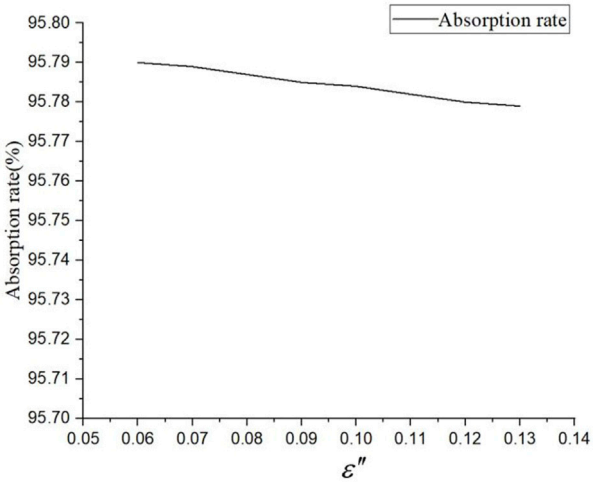

FIGURE 9
Variation in the energy-absorption rate when changing the imaginary part of the relative permittivity.

$$\mathrm{RA} = \frac{P}{P_{in}}$$

where P and P_{in} are the power absorption of heat-absorbing material and port input power, respectively. As absorption rate increases, the power absorption of load increases. Absorption rate have a range between 0 and 100%.

The radiation of the electric field was determined by the resonance of the slot and interference of the current. Slot resonance occurs when the length of the slot is half the wavelength. When resonance occurs, an electric field radiates from the slot. Typically, slots can be designed as vertical or horizontal slots and arranged with adjacent columns or rows spaced at half the wavelength.

The vertical and horizontal slot arrangements (Figure 3, 4) resulted in poor and better heating effects Table 2, respectively. As the average body temperature increased, the COV was optimized from 0.371 to 0.305 and the absorption rate was improved by 13%. By comparing the two slot arrangements, it can be observed that the use of a horizontal slot arrangement can effectively improve uniformity and heating efficiency.

3.2 The effect of staggered slot arrangement on microwave heating

The heating effect of the staggered slot arrangement (Figure 5) is shown in Figure 6, which demonstrates the heating effects for the horizontal distance of $\lambda_g/2$ between the centers of the adjacent rows (columns) of the slots.

In Table 3, we found that the staggered slot arrangement had a higher average body temperature than the uniform slot arrangement, and the COV was optimized from 0.305 to 0.28,

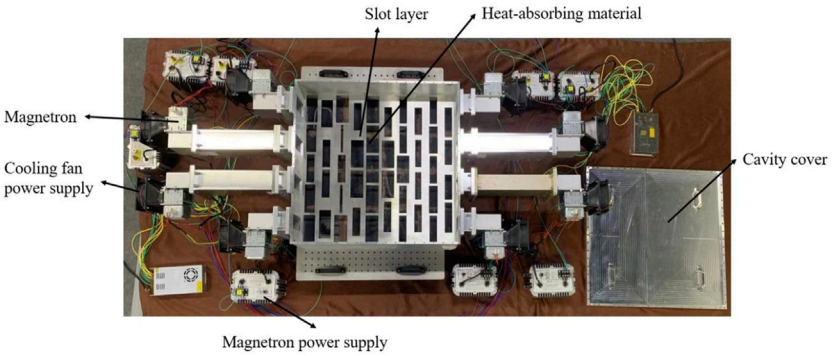

FIGURE 10
Experimental setup system.

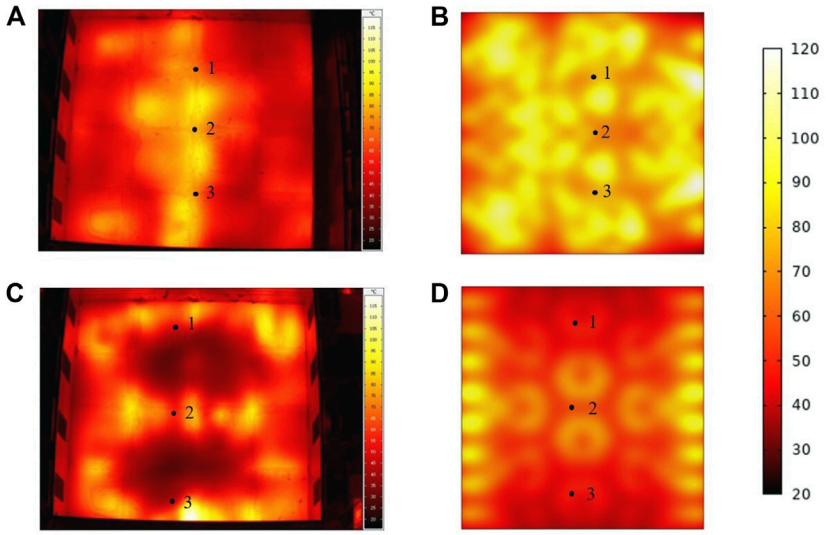

FIGURE 11
Comparison of the simulation and experimental results. **(A)** Experimental and **(B)** simulation results with a slotted layer and **(C)** experimental and **(D)** simulation results without a slotted layer.

with a 55.6% increase in energy absorption. Therefore, the use of a staggered slot arrangement can effectively improve uniformity and heating efficiency.

3.3 Optimization of slot size

We used a genetic algorithm to optimize the slot size. The length and width of the slots were used as optimization parameters, the COV was used as an indicator, and a corresponding fitness function was constructed. First, the structure was parametrically encoded and mapped into the form of individual codes that can be processed using a genetic algorithm. An initial population containing a certain number of individuals was generated, wherein each individual represents one type of slot arrangement. COMSOL was used to numerically calculate the model, and the obtained data were entered into a fitness function to calculate the fitness function value. After iterative optimization, the optimal individuals were selected, crossed over, and mutated to produce the next generation of populations. This process was repeated until the set targets were achieved.

Based on Figure 7, 8, the average temperature of the optimized slot arrangement increases, COV is optimized from 0.28 to 0.22, uniformity is significantly improved, and the energy-absorption rate is increased by 8.1%, compared to the non-optimized slot arrangement, as can be seen in Table 4. Hence,

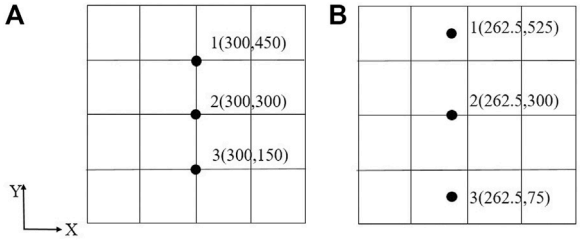

FIGURE 12
Location for temperature measurement **(A)** with slotted layer **(B)** without slotted layer.

it is proven that the heating uniformity and efficiency of the optimized slot arrangement are significantly better than those of the non-optimized slot arrangement. Thus, we used an optimized slot arrangement in the experiment.

3.4 Robustness analysis

3.4.1 Robustness analysis of the slot size (length and width)

To study the robustness of the slot, we used the range of variation in the energy-absorption rate to evaluate the robustness. For the slot width and length parameters, we performed an overall increase or decrease of 1 mm and subsequently observed the range of variation in the energy-absorption rate and determined the robustness.

From the data presented in Tables 5 and 6, it can be concluded that the variation in the energy-absorption rate of the slot was less than 1% when the overall slot width parameter was increased or decreased by 1 mm. The variation in the energy-absorption rate was less than 2% when the overall length of the slot was increased or decreased by 1 mm. In summary, the robustness of the system was good.

3.4.2 Robustness analysis of the material parameters

For the heat-absorbing material, the range of variation in the energy-absorption rate was determined by increasing or decreasing the imaginary part of the relative permittivity by 50%. From Figure 9, it can be concluded that the change in the energy-absorption rate is less than 0.1% and the robustness is good.

3.5 Simulation and experimental comparison

3.5.1 Experimental setup

The experimental setup system, which was used to verify the simulation, is shown in Figure 10. The magnetrons (Panasonic 2M244-M1) were powered by eight power supplies (WepeX 1280A-HN), while the fan (AVC 2B12038B24H) is mounted on the side of the magnetron. Microwave energy was fed into the cavity through eight ports. The top of the cavity was a metal cover and the heat-absorbing material was placed below the slot layer; thus, the surface temperature of the internal heat-absorbing material could be measured by opening the top cover and pulling out the slot layer after heating is completed.

3.5.2 Experimental procedures

The actual heating process is driven by eight magnetron power supplies to supply microwaves. A fan is turned on to dissipate heat from the magnetrons. Both walls of the chamber are slotted for easy insertion of the metal slot layer. At 2.45 GHz, 800 W of power was used to heat the heat absorbing material placed at the bottom for 120 s. After heating, the top lid of the cavity was opened within 10 s and the final temperature distribution on the top surface was measured by a thermal imager (VarioCAM hr inspect500, InfraTec., Dresden, Germany) within 30 s.

TABLE 7 Temperature comparison between experiment and simulation with slotted layer at different positions.

Position	Experimental temperature (°C)	Simulation temperature (°C)	Temperature difference (°C)
1	70.2	74.8	−4.6
2	78.7	75.7	3.0
3	75.4	77.9	−2.5

TABLE 8 Temperature comparison between experiment and simulation without slotted layer at different positions.

Position	Experimental temperature (°C)	Simulation temperature (°C)	Temperature difference (°C)
1	40.7	44.0	−3.3
2	54.0	53.0	1.0
3	40.3	41.0	−0.7

3.5.3 Experimental results

The comparison of the simulation and experimental results is shown in Figure 11. In (a) and (b), we took three specific positions in the experimental results as shown in Figure 12A, compared their temperatures at the same positions in the simulation results, and summarized the temperature differences, as shown in Table 7. The experimental data were post-processed by the data obtained from the thermal imager, and the data were analyzed for errors and the average value of multiple measurements was obtained. The temperature differences at the three locations are −4.6, 3, and −2.5 (°C), and their absolute values are all less than 5 (°C). Then compare the experimental and simulation results without metal layer. As shown in (c) and (d), we took three specific positions in the experimental results as shown in Figure 12B, compared their temperatures at the same positions in the simulation results, and summarized the temperature differences. As shown in Table 8, the temperature differences at the three positions are −3.3, 1, −0.7 (°C), the absolute value of which is less than 5 (°C). Therefore, by comparing the simulation with the experimental temperature distribution, it is concluded that the simulation and the experiment have a good agreement.

4 Summary

In this study, a microwave heating multi-generator cavity was designed, wherein a metal slot layer was placed inside the cavity to make the energy radiation uniform, to improve the heating uniformity and efficiency. The effects of the slot arrangement on the microwave heating uniformity in the multi-generator cavity were discussed and the size of the slot was optimized. The results indicated that the optimized metal slot improved the heating uniformity of the cavity, with the heating efficiency reaching 95%. The optimized size of the slot and the parameters of the heat-absorbing material were analyzed for robustness, and the results showed that the variation in the energy-absorption rate did not exceed 2% when the slot size was varied within 1 mm. Furthermore, the variation in the energy-absorption rate did not exceed 0.1% when the permittivity of the material in the imaginary part was varied in the range of 50%. Finally, experiments were conducted to verify the accuracy of the simulation results of the optimized metal slot; the experimental results were found to be in good agreement with the simulation results.

Data availability statement

The original contributions presented in the study are included in the article/Supplementary Material, further inquiries can be directed to the corresponding author.

Author contributions

SY conceived and modeled the model, and verified the model through experiments. Process the data and write the first draft.

Acknowledgments

Thanks to Sichuan University for providing COMSOL Multiphysics software, as well as the experimental site and instruments.

Conflict of interest

The authors declare that the research was conducted in the absence of any commercial or financial relationships that could be construed as a potential conflict of interest.

Publisher's note

All claims expressed in this article are solely those of the authors and do not necessarily represent those of their affiliated organizations, or those of the publisher, the editors and the reviewers. Any product that may be evaluated in this article, or claim that may be made by its manufacturer, is not guaranteed or endorsed by the publisher.

References

Ahn, S. H., Jeong, C. H., and Seo, D. G. (2019). "Improved heating uniformity of a 3-kWatt 2.45GHz microwave dryer using multiple multi-slotted waveguides," in *International applied computational electromagnetics society symposium (ACES)*, 1–2.

Ahn, S., Jeong, C., Lim, D., and Lee, W. (2020). Kilowatt-level power-controlled microwave applicator with multiple slotted wave-guides for improving heating uniformity. *IEEE Trans. Microw. Theory Tech.* 68, 2867–2875. doi:10.1109/TMTT.2020.2977645

Bae, S.-H., Jeong, M.-G., Kim, J.-H., and Lee, W.-S. (2017). A continuous power-controlled microwave belt drier improving heating uniformity. *IEEE Microw. Wirel. Compon. Lett.* 27, 527–529. doi:10.1109/LMWC.2017.2690849

Cai, C., Ge, T., Zhang, M., Zhao, Y., Wu, C., and Han, J. (2021). Effect on combustion properties of coal treated by microwave irradiation combined with sodium hydroxide solution. *Processes* 9, 1284. doi:10.3390/pr9081284

Chen, J. H., Althaus, S. M., Liu, H. H., Zhang, J. L., Eppler, G., Duncan, J. C., et al. (2021). Electromagnetic-heating enhancement of source rock permeability for high recovery. *Fuel* 283, 118976. doi:10.1016/j.fuel.2020.118976

Cuccurullo, G., Giordano, L., Metallo, A., and Cinquanta, L. (2017). Influence of mode stirrer and air renewal on controlled microwave drying of sliced zucchini. *Biosyst. Eng.* 158, 95–101. doi:10.1016/j.biosystemseng.2017.03.012

Dinani, S. T., Kubbutat, P., and Kulozik, U. (2020). Assessment of heating profiles in model food systems heated by different microwave generators: Solid-state (semiconductor) versus traditional magnetron technology. *Innovative Food Sci. Emerg. Technol.* 63, 102376. doi:10.1016/j.ifset.2020.102376

Geedipalli, S. S. R., Rakesh, V., and Datta, A. K. (2007). Modeling the heating uniformity contributed by a rotating turntable in microwave ovens. *J. Food Eng.* 82, 359–368. doi:10.1016/j.jfoodeng.2007.02.050

Gu, H., Ye, J. H., Wang, G., Yan, X. T., Zhu, H. C., and Yang, Y. (2022). Effects of metal boundary stretching and sample translational motion on microwave heating. *Processes* 10, 246. doi:10.3390/pr10020246

Hartlieb, P., Kuchar, F., Moser, P., Kargl, H., and Restner, U. (2018). Reaction of different rock types to low-power (3.2 kW) microwave irradiation in a multimode cavity. *Miner. Eng.* 118, 37–51. doi:10.1016/j.mineng.2018.01.003

Hassani, F., Nekoovaght, P. M., and Gharib, N. (2016). The influence of microwave irradiation on rocks for microwave-assisted under-ground excavation. *J. Rock Mech. Geotechnical Eng.* 8, 1–15. doi:10.1016/j.jrmge.2015.10.004

He, J., Yang, Y., Zhu, H., Li, K., Yao, W., and Huang, K. (2020). Microwave heating based on two rotary waveguides to improve efficiency and uniformity by gradient descent method. *Appl. Therm. Eng.* 178, 115594. doi:10.1016/j.applthermaleng.2020.115594

Khelfa, A., Rodrigues, F. A., Koubaa, M., and Vorobiev, E. (2020). Microwave-Assisted pyrolysis of pine wood sawdust mixed with Ac-tivated carbon for bio-oil and bio-char production. *Processes* 8, 1437. doi:10.3390/pr8111437

Kumar, S. N., Grekov, D., Pre, P., and Alappat, B. J. (2020). Microwave mode of heating in the preparation of porous carbon materials for adsorption and energy storage applications - an overview. *Renew. Sustain. Energy Rev.* 124, 109743. doi:10.1016/j.rser.2020.109743

Li, C. N., Lin, X. Q., Liu, D. Y., and Wen, Z. (2020). Regionally tunable microwave heating technology using time-frequency-space domain synthesis modulation method. *IEEE Trans. Ind. Electron.* 68, 10240–10247. doi:10.1109/TIE.2020.3026295

Li, H., Zheng, C., Lu, J., Tian, L., Lu, Y., Ye, Q., et al. (2019). Drying kinetics of coal under microwave irradiation based on a coupled electromagnetic, heat transfer and multiphase porous media model. *Fuel* 256, 115966. doi:10.1016/j.fuel.2019.115966

Liao, J., Mo, Q., Li, C., Han, Y., Chang, L., and Bao, W. (2019). Classification of water forms in lignite and analysis of energy consumption on the drying processes by microwave and fixed bed. *Fuel* 253, 580–587. doi:10.1016/j.fuel.2019.05.047

Lichao, G., and Xiaoyan, L. (2022). The interaction between microwave and coal: A discussion on the state-of-the-art. *Fuel*, 314, 123140. doi:10.1016/j.fuel.2022.123140

Luan, D., Tang, J., Pedrow, P. D., Liu, F., and Tang, Z. (2016). Analysis of electric field distribution within a microwave assisted thermal sterilization (MATS) system by computer simulation. *J. Food Eng.* 188, 87–97. doi:10.1016/j.jfoodeng.2016.05.009

Razmhosseini, M., and Vaughan, R. G. (2017). "Impedance bandwidth of a slotted waveguide array: Impact of waveguide length and element shape," in *Proceedings of the international symposium of IEEE-antennas-and-propagation-society /USNC/URSI national radio science meeting* (San Diego, CA, 1587–1588.

Shan, X. (2020). Research progress in the application of microwave technology in environmental treatment. *Saf. Environ. Health* 20, 33–37.

Shen, L., Gao, M., Feng, S., Ma, W., Zhang, Y., Liu, C., et al. (2022). Analysis of heating uniformity considering microwave transmission in stacked bulk of granular materials on a turntable in microwave ovens. *J. Food Eng.* 319, 110903. doi:10.1016/j.jfoodeng.2021.110903

Si, C., Wu, J., Zhang, Y., Liu, G., and Guo, Q. (2019). Experimental and numerical simulation of drying of lignite in a microwave assisted fluidized bed. *Fuel* 242, 149–159. doi:10.1016/j.fuel.2019.01.002

Suhail, N. A., Kok, Y. Y., Chong, C. Y., El-Enshasy, H. A., Mohamed Ali, M. S., Zainol, N. A., et al. (2022). Optimisation of heating uniformity for milk pasteurisation using microwave coaxial slot applicator system. *Biosyst. Eng.* 215, 271–282. doi:10.1016/j.biosystemseng.2022.01.013

Taheri-Shakib, J., and Kantzas, A. (2021). A comprehensive review of microwave application on the oil shale: Prospects for shale oil production. *Fuel* 305, 121519. doi:10.1016/j.fuel.2021.121519

Tang, Z., Hong, T., Liao, Y., Chen, F., Ye, J., Zhu, H., et al. (2018). Frequency-selected method to improve microwave heating performance. *Appl. Therm. Eng.* 131, 642–648. doi:10.1016/j.applthermaleng.2017.12.008

Wang, C., Yao, W., Zhu, H., Yang, Y., and Yan, L. (2021). Uniform and highly efficient microwave heating based on dual-port phase-difference-shifting method. *Int. J. RF Microw. Comput. Aided. Eng.* 31, 9. doi:10.1002/mmce.22784

Wang, Y., Yang, X., and Qiu, Y. (2021). Double pendulum mode stirrer for improved multimode microwave heating performance. *Int. J. RF Microw. Comput. Aided. Eng.* 31, 11. doi:10.1002/mmce.22866

Wu, Y., Lan, J., Yang, F., Hong, T., Yang, Y., Zhu, H., et al. (2021). Study of the high heating efficiency and uniformity by multi-port sweep frequency microwave irradiations. *J. Microw. Power Electromagn. Energy* 55, 316–332. doi:10.1080/08327823.2021.1993044

Yang, F., Wang, W., Yan, B., Hong, T., Yang, Y., Zhu, H., et al. (2019). Sweep frequency heating based on injection locked magnetron. *Process. (Basel).* 7, 341. doi:10.3390/pr7060341

Ye, J., Lan, J., Xia, Y., Yang, Y., Zhu, H., and Huang, K. (2019). An approach for simulating the microwave heating process with a slow- rotating sample and a fast-rotating mode stirrer. *Int. J. Heat Mass Transf.* 140, 440–452. doi:10.1016/j.ijheatmasstransfer.2019.06.017

Ye, J., Xia, Y., Yi, Q., Zhu, H., Yang, Y., Huang, K., et al. (2021). Multiphysics modeling of microwave heating of solid samples in rotary lifting motion in a rectangular multi-mode cavity. *Innovative Food Sci. Emerg. Technol.* 73, 102767. doi:10.1016/j.ifset.2021.102767

Yucen, K., Shuangshuang, C., Zhang, L., and Zhang, S. (2022). Transformation behaviour of pyrite during microwave desulfurization from coal: Phase and structural change of Fe-S compounds. *Fuel* 316, 123284. doi:10.1016/j.fuel.2022.123284

Zhu, J., Li, X., Yang, Z., Zhou, J., and Wang, H. (2022). Drying characteristics of oil shale under microwave heating based on a fully coupled three-dimensional electromagnetic-thermal-multiphase transport model. *Fuel* 308, 121942. doi:10.1016/j.fuel.2021.121942

Zhu, J., Yi, L., Yang, Z., and Li, X. (2021). Numerical simulation on the *in situ* upgrading of oil shale reservoir under microwave heating. *Fuel* 287, 119553. doi:10.1016/j.fuel.2020.119553